Scientific publication submitted to:

Wood Material Science and Technology ISSN (Online): 1748-0280

BENDING BEHAVIOUR OF CLT STRESSED SKIN PANELS MANUFACTURED WITH MOUNTAIN PINE (*Pinus uncinata* Ramond ex DC.)

Luengo, E.[1,2,3]; Gilabert-Sanz, S.[4]; Oliver-Villanueva, J.V.[5]; Osuna, C.[6]; Hermoso, E. [6]

[1] Department of Forestry and Environmental Engineering and Management, MONTES (School of Forest Engineering and Natural Resources), Universidad Politécnica de Madrid, 28040 Madrid, Spain
[2] Continuum Mechanics and Structural Analysis Department, Universidad Carlos III de Madrid, 28911 Madrid, Spain
[3] AITIM—Technical Research Association for the Wood Industries, 28013 Madrid, Spain
[4] Department of Architectural Representation, Universitat Politècnica de Catalunya, 08028 Barcelona, Spain. ORCID 0000-0001-9035-6649
[5] UPV-ITACA Research Institute, Universitat Politècnica de València, 46022 Valencia, Spain. ORCID 0000-0003-2842-7834
[6] Institute of Forest Science (ICIFOR-INIA, CSIC), 28040 Madrid, Spain

ABSTRACT

Cross Laminated Timber (CLT) elements are wood-based structural products in world-wide expansion. However, its structural application as a bending element implies the use of important amount of wood as raw material when compared to other floor solutions such as those used in light framing. For that reason, research is being carried out to obtain alternative CLT floor and roof elements with a more favourable ratio of wood amount to stiffness.

In this research a new construction system has been designed and tested using thin CLT skins and finger-jointed wood stringers of mountain pine (*Pinus uncinata* Ramond ex DC.) as an example of an alternative raw material in Southwestern Europe to increase the added value of scarce forest products. Also, it was considered as an additional objective to assess its combined use with cork insulation materials, obtaining fully natural renewable building products that can be used to improve energy efficiency in buildings. To fulfil these objectives two different types of stressed-skin panels were designed for roof and floor uses, manufactured, and tested in bending, obtaining key mechanical performance information assessing the use of the gamma method for their design and evaluating their efficiency in the use of wood compared with CLT elements with similar stiffness.

The main results obtained demonstrate that the SSPs based on CLT of *Pinus uncinata* timber show adequate mechanical values for the expected mechanical performance, both for roof elements and floor construction elements. Furthermore, the designed and tested SSP-CLT shows similar stiffness in comparison with other CLT elements, by saving wood and increasing material efficiency. Finally, this result will allow valorising and wisely using this alternative resource, promoting at the same time the development of the forest areas in which *Pinus uncinata* species is growing. Finally, this innovative prefabricated system of panels also opens the possibility to incorporate cork as natural and renewable insulation material, contributing

to the development of local economies in rural less-favoured regions in Southwestern Europe based on sustainable wood-based construction.

KEYWORDS

Cross Laminated Timber CLT; Stressed Skin Panels SSP; Mountain pine - *Pinus uncinata*; mechanical behaviour; renewable raw materials; efficient use of wood

1. INTRODUCTION

Mountain Pine (*Pinus uncinata* Ramond ex DC.) is an autochthonous species found naturally in mountain ranges of Spain, France and Central Europe (López-Díez et al. 2011), being one of the tree species that grow in the highest altitudes, enduring harsh winter conditions but needing a minimum rainfall during all the periods of the year (Corona et al. 2015). The Pyrenees is one of the main areas in which it dominates forest mountain ecosystems, normally between 1,700 and 2,500 m.o.s.l. (Cantegrel 1981). Due to the difficult stand situation and habitat singularity, *Pinus uncinata* is not normally considered as a production species, being its main value the ecological and protective function (LIFE21-NAT-ES-LIFE UNCINATA (2023). However certain wood production is available and increasing locally, mainly in the Eastern Pyrenees, being traditionally used for rustic building and overhead line poles, considering its use interesting as a mean for rural development, especially for sustainable construction with high added value.

Due to the relatively low use of mountain pine timber for structural purposes, the standardization of its visual strength grading is still in progress . Thus, bending testing, grading analysis and machine grading analysis for sawn timber based on NF-B 52-001 (2011) have been already performed in France (Burgers et al. 2019). These tests show an average modulus of elasticity (MOE) of 9,076 N/mm^2 , with the two intermediate grades of MOE assessment ranging between 8,381 and 9,876 N/mm^2. Moreover, other unpublished tests have been made in the framework of the European Project UNCI'PLUS (2011), applying timber grading standards UNE 56544 (2011) and NF-B52-001 (2011) in Spain and France, respectively. This study indicates that for these national grading standards the average strength classes obtained (ME2-MEG and STII-STIII) can be assigned to a C16-C18 strength grade following EN 338 (2016), while the best strength classes obtained (ME-1 and STI) can be assigned to C22.

Although Cross Laminated Timber (CLT) has shown to be a very interesting and successful building product (De Araujo et al. 2023), its use as a bending structural element is sometimes considered controversial, as the amount of wood necessary to obtain the required stiffness is high when compared to other floor solutions such as those used in light framing. Today, the available technology for manufacturing CLT panels allows to successfully manufacture and press Stressed Skin Panels (SSP) with large length dimensions (from 6 to 12 m, and even longer) (Luengo et al. 2017). This provides a unique opportunity for large prefabricated elements with continuous flanges and stringers. Furthermore, improving classical SSP structural panels formed with wood-based panels flanges glued to ribs or stringers, big sized SSP have been recently developed using Laminated Veneer Lumber (LVL) or CLT flanges and LVL or Glued Laminated Timber (GLT) ribs, mainly using spruce wood (*Picea abies* L.) (Darzi et al 2020; Santos et al., 2021).

More research and testing is necessary to generate scientific and technical knowledge on the bending behaviour of these new products. For example, Stanić et al. (2016) assessed an optimization procedure for an economic design of a CLT plate with stiffening ribs using also numerical models for its design. Luengo et al. (2017) studied the influence on properties of the bonding control of radiata pine (*Pinus radiata* D.Don) CLT double faced ribbed panels, compared with the stresses expected in the gluelines between the stringers and the flanges. Lavrencic and Brank (2018) assessed failure processes in CLT ribbed panels using testing and numerical modelling to estimate the limit load and displacement on such elements. Choi et al. (2018) evaluate the bending strength of CLT with Korean larch (*Larix kaempferi* Carr.) plywood. Shahnewaz et al. (2022) studied the vibration and flexural performance of CLT-GLT composite panels assessing different types of connectors, and vibration tests in bending with acceptable results. Furthermore, other authors research the combination of CLT with other materials for product optimization in different construction solutions. For example, Loss and Davidson (2017) combined cold formed steel beams with CLT, joining them using bolts and screws. Additionally, Munis et al. (2018), Dong et al. (2021) and Wei et al. (2021) tested CLT elements reinforced with bamboo stripes, and Santos et al. (2021) tested polyurethane rigid foam cored CLT sandwich panels.

Moreover, the use of agglomerated or expanded cork (*Quercus suber* L.) as an insulation ultralight material in loadbearing panels has been explored in the commercial fabrication of solid wood lamellas or SWP faced sandwich panels, and also in research of new sandwich panel types (Hami et al. 2014, Lakreb et al. 2018), but so far no results have been published for CLT based sandwich panels.

In order to achieve the main objectives, this we designed two types of stressed-skin panels (SSP) with thin CLT faces, also looking for solutions in which the insulation material is cork as a natural, renewable and locally produced forest product. Prototypes of both SSPs were manufactured using locally obtained mountain pine wood in the region surrounding the manufacturing facilities in Catalonia (Spain), thus reducing the transport logistics. Full-scale testing was considered necessary, since the available official design methods for SSP (EN 1995-1-1 (2004+AC:2006+A1:2008+A2:2014) were developed mainly for elements with uniform and thin flanges, such as those manufactured with plywood or OSB. Therefore, some aspects of the calculations, such as effective flange width and shear deformation of the faces, remain unclear for CLT faced panels, requiring testing and analysis with models. To do this, the gamma method adapted to CLT design (Gagnon and Popovski 2011) was considered for comparison.

This research is included in a wider research and development project (IMIP 2023) focused in improving the available building solutions manufactured with renewable natural products in the Southwest of Europe (Brunet-Navarro et al. 2020).

2. MATERIALS AND METHODS

2.1. Panels design and manufacturing

Two types of SSP prototypes were designed:

- A PANEL: 6 m long and 1.2 m wide roof element composed by a lower single three layered CLT skin with 4 finger-jointed wood ribs glued on the top (Figure 1).
- C PANEL: 6 m long and 1.2 m wide floor element composed by an upper and lower three layered CLT skins glued to a central web of 4 finger-jointed wood ribs (Figure 2).

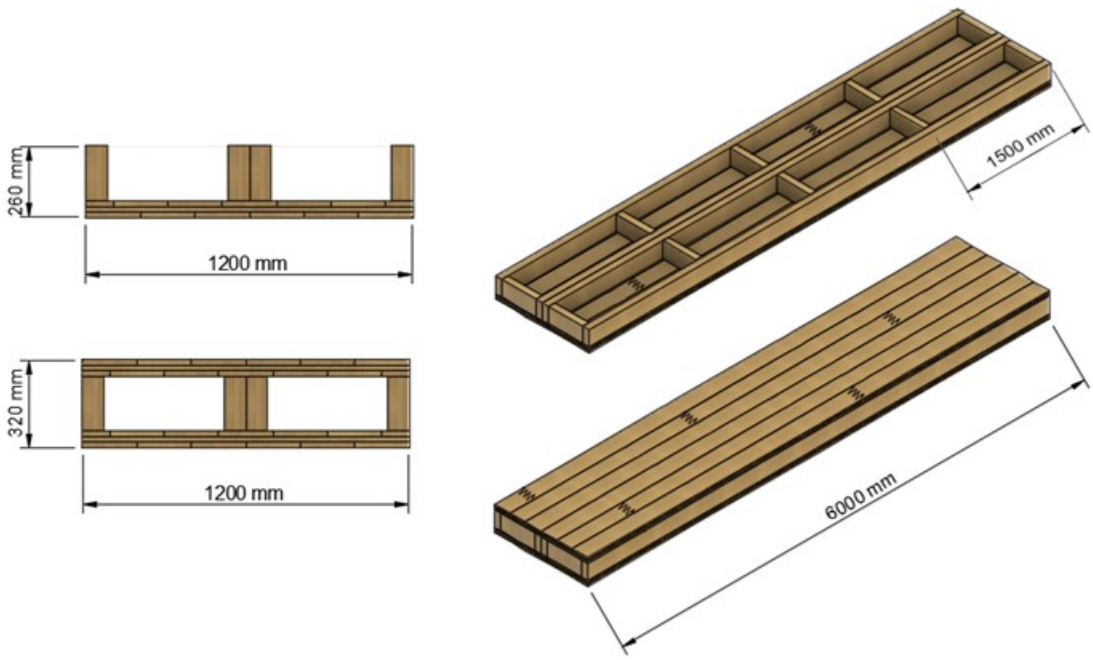

Figure 1. Sections and plans of the panels. Above, A panel type (roof element); below, C panel type (floor element).

Figure 2. Manufactured full size C panel

The panels were designed using a double rib in the central position and a single rib in the lateral position (Figure 1) in order to obtain floor or roof elements with uniform stiffness. Thus, once the panel is installed, a double rib is repeated as the structural element in the web. Transversal short boards (like the longitudinal ribs) were also included for closing the panel cavities, providing lateral stability for manufacturing and structural purposes. The panels were pre-designed for bending in simply supported situation using the gamma method adapted to CLT ribbed panels in order to define the basic characteristics, such as the rib's height and the maximum span required to fulfil the deflection requirements in a roof and floor situation, according to the Spanish reference documents DB-SE-AE (2009), and DB-SE (2019).

The mountain pine timber for CLT skins of the panels was visually graded as a ME2 quality according to UNE 56544 (2022) and finger-jointed using a PUR structural Type I adhesive according to EN 15425 (2017). The final product having three layers of 20 mm, with a total thickness of 60 mm. The ribs were also manufactured using wood of the same species an origin graded as a MEG quality of UNE 56544 (2022) standard, i.e., C18 following EN 338 (2016). For the and finger-joint we used the same adhesive as in the CLT lamellas manufacturing, having a final cross-section of 80 x 200 mm. So, the skins were glued to the ribs also using a PUR structural Type I adhesive, according to EN 15425 (2017). Finally, the panels were individually pressed with a vacuum-press, following EN 16351 (2021). All the manufacturing processes, as well as the timber supply, was carried out by a small local sawmill located close to the forest resources in Lleida, Catalonia (Spain).

Two types of cork insulation materials were used accordingly to the characteristics of the stressed-skin panels:

- expanded and agglomerated black-cork boards (ICB of 110-120 kg/m^2, according to EN 13170) for open panels to be used in roofs (A PANEL),
- and granulated cork particles (0.5-1.5 mm, according to UNE 56920), for closed-box panels to be used in floors (C PANEL).

However, since the cork insulation do not have any active role in the mechanical behaviour of the panels, specific specimens without insulation were manufactured for the bending tests.

2.2. Test specimens

Six full size panels of each type (A and C), were used for bending tests in its full length in the lab. The panels were sectioned obtaining two types of specimens of 593 mm of width (Figures 3 and 4), in order to study their behaviour in the central and lateral ribs. This has been done considering that the differences in the CLT continuity in both panels can lead to a different shear stress distribution in the most stressed areas and can consequently originate differences in the failure load.

- A specimen type including the central two ribs with CLT continuity in the centre of flange/s, named as SPECIMEN TYPE I.
- A specimen type formed adjoining the two lateral ribs, with no CLT continuity in the centre of the flange/s, named as SPECIMEN TYPE II, of which two subtypes were defined:
    - SPECIMEN SUBTYPE IIa, of simply adjoined parts, only clamped laterally in the support area to avoid lateral movements of the section.
    - SPECIMEN SUBTYPE IIb, of adjoined parts screwed at 45° in the upper part of the panels. This is used to analyse if any additional effect can be detected because of the lateral interlocking of the panels.

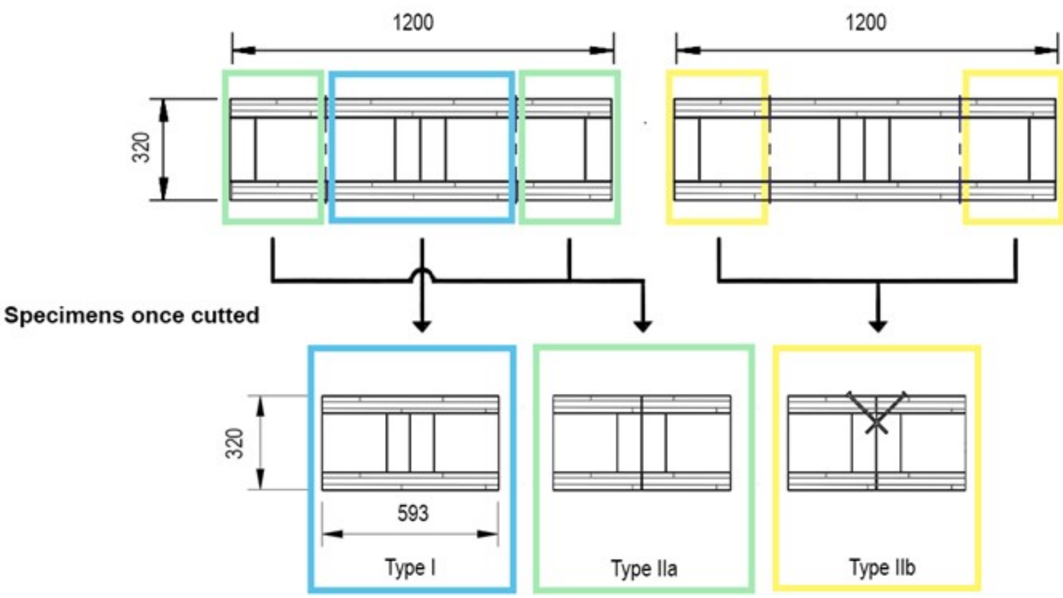

Figure 3. Example of C panels adjoined, in section and specimen component position.

Figure 4. Type I specimens

Although cutting specimens from the original panels can lead to miss some information on the effects of the stress distribution in the flange in the areas situated in the middle zone between the ribs, this effect was considered of lesser importance compared to the analysis of the most stressed zones such as the ones situated in the contact area between the flanges and the stringers. Also, the tested situation was equal or more critical than the one in the entire panels, and therefore valid for a preliminary analysis. Table 1 describe the specimens' number of each type finally tested.

Table 1. Panels and specimens tested

Panel type	Reference panels used	Total no. of type I spec.	Total no. of type IIa spec.	Total no. of type IIb spec.
A	1, 2, 3	3	3	
	4, 5, 6			3
C	7, 8, 9	3	3	
	10,11,12			3

Type IIb specimens were screwed as is shown Figure 3, using two pairs of structural screws with a length of 230 mm and a head diameter of 10 mm, each pair screwed at 45° in opposite members (Figure 5).

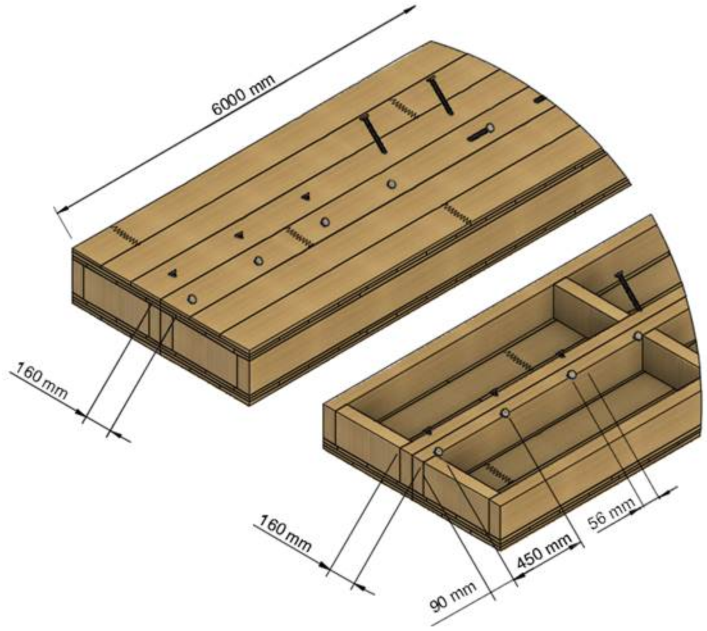

Figure 5. Type IIb specimens joining using inclined screwing.

2.3. Test methods

The specimens were tested in 4-point bending test in its full length, with a span of 5,920 mm, which is the expected span for the panels in its final use according to the EN 408 (2010+A1:2012) (Figure 6). The A panels were tested in a slightly longer span of 23 times the height of the specimen (EN 408 recommends a minimum of 18 times), as the purpose was to test the product in its intended service span. The tests offer results of failure load and mode as well as the global load-deflection rate measured at the centre of the span in the lower skin of the panel.

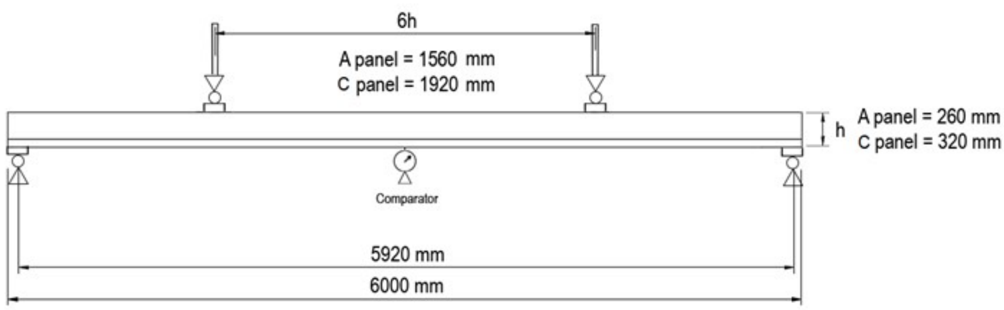

Figure 6. Loads and supports arrangement in 4-point bending test

The bending stiffness and bending moment were obtained according EN 408 (2010). Additionally bending shear was calculated with following equations (1), (2) and (3):

- Bending stiffness:

$$E \cdot I = \frac{3 \cdot a \cdot \ L^2 - 4 \cdot a^3}{48 \cdot \left(\frac{\Delta w}{\Delta F}\right)} \ (kN \cdot m^2) \tag{1}$$

Where:
E: is the modulus of elasticity in $kN \cdot mm^{-2}$;
I: is the moment of inertia in mm^4;
a: is the distance between the lower and upper support in m;
L: is the span length in mm;
$\Delta w/\Delta F$: is the slope obtained from the force-deformation curve in $mm \cdot kN^{-1}$.

- Bending moment:

$$M = \frac{a \cdot F_{max}}{2} \ (kN \cdot m) \tag{2}$$

Where:
a: is the distance between the lower and upper support in m;
F_{max}: is the maximum load at failure in kN.

- Bending shear:

$$f_v = \frac{F_{max}}{2} \ (kN) \tag{3}$$

Where:
F_{max}: is the maximum load at failure in kN.

2.4. Modelling of the bending stiffness

A variation of the gamma method for CLT elements was developed and applied to compare the experimental results with currently available models for CLT elements as well as to assess the results of this modelling using the specimen width as the effective flange width. This methodology has the particularity of modelling a 7-layer CLT, where the three central layers are modelled as a substitution of a double T-section including two longitudinal beams and two adjacent layers. The calculation of the moment of inertia of the composite section is obtained with the Steiner's theorem (4).

$$I_{total} = I_{l,1} + \ I_{l,2} + \ I_{l,3} \tag{4}$$

Where:
I_{total}: It is the moment of inertia of the composite section in mm^4
$I_{l,i}$: It is the moment of inertia of each of the layers in mm^4. Layer 1 is the bottom layer and layer 3 is the top layer of CLT. Layer 2 is the two longitudinal beams.

Therefore, the moment of inertia can be calculated with the following Equation (5).

$$I_{l,i} = \frac{b_i \cdot t_i^3}{12} + b_i \cdot t_i \cdot a_i^2 \quad (5)$$

Where:
b_i: is the total width of the layer in mm.
t_i: is the thickness of the layer in mm.
a_i: is the distance from the centre of the face to the neutral axis in mm.

To calculate the stiffness of the composite panel, the moment of inertia obtained shall be multiplied by the MOE of the t-panel ($E_{t\text{-}panel} \cdot I_{total}$).

The 7-layer panel is calculated following the calculation of a 5-layer panel, where the central layer has a greater thickness, equal to the height of the 3-layer composite panel. In this case, as the panel is symmetrical, the model can be simplified by using the equations (6) to (9). Moreover, equations (8) and (9) calculate the value of γ_1, γ_2 and γ_3.

$$E \cdot I = (E_1 \cdot I_1 + \gamma_1 \cdot E_1 \cdot A_1 \cdot a_1^2) + (E_2 \cdot I_2) + (E_3 \cdot I_3 + \gamma_3 \cdot E_3 \cdot A_3 \cdot a_3^2); \quad (6)$$

$$E \cdot I = E \cdot [(I_1 + \gamma_1 \cdot A_1 \cdot a_1^2) + I_2 + (I_3 + \gamma_3 \cdot A_3 \cdot a_3^2)] \quad (7)$$

$$\gamma_2 = 1; \quad (8)$$

$$\gamma_1 = \gamma_3 = \frac{1}{1 + \frac{\pi^2 \cdot E \cdot A}{L^2} \cdot \frac{\bar{h}}{G_R \cdot b}} \quad (9)$$

Where:
$E \cdot I$: it is the 7-layer panel bending stiffness in N mm^{-2};
$E_i \cdot I_i$: they are the bending stiffness of each layer from below to above (i = 1 to i =3) in N mm^{-2};
A_i: it is the cross-sectional area of each layer in mm^2;
γ_i: it is the gamma coefficient of each layer;
L^2: it is the length of the panel in mm;
$\bar{h}$: it is the thickness of the transverse layer adjacent to the longitudinal layer in mm;
G_R: it is the shear modulus in N mm^{-2};
b: it is the width of the layer in mm.

Finally, C panel bending stiffness is obtained following the 5-layer simulation by subtracting the central thick layer and adding the one calculated for the core, as explained in equation (10). Figure 7 shows the calculation process in a simplified way.

$$E_c \cdot I_c = E \cdot I - E_2 \cdot I_2 + E_{t-panel} \cdot I_{total} \quad (10)$$

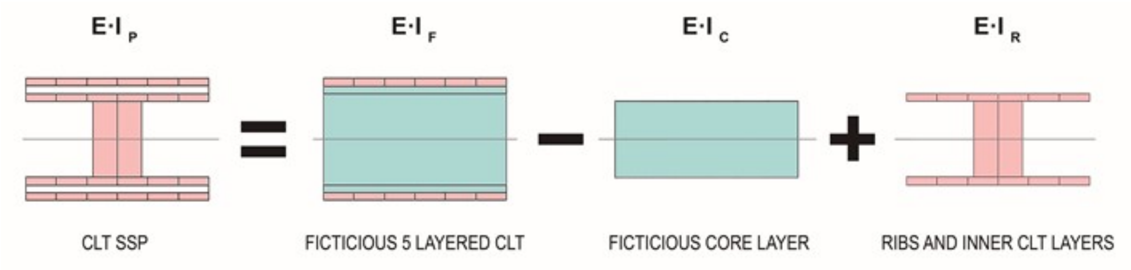

Figure 7. Process of calculation an equivalent 7-layer CLT to C panel via the method.

3. RESULTS AND DISCUSSION

3.1. Bending tests results

Tables 2 and 3 show the results for bending tests of A and C panels, respectively.

Table 2. Test results for the A panels specimens

Spec. type	No. of tests	E.I eff (kN/mm^2) Average value	E.I eff (kN/mm^2) Range[a]	Max. Bending moment at failure (kN.m) Average value	Max. Shear force at failure (kN) Average value	Failure mode
I	3	3236134283	599284908	87.1	40.0	Shear 33% Bending 67%
IIa	3	3305452116	47341442	96.6	44.3	Bending 100%
IIb	3	3196667598	298293801	82.7	37.9	Shear 100%

[a] Range: difference between the maximum and minimum values obtained.

Table 3. Test results for the C panels specimens

Spec. type	No. of tests	E.I eff (kN/mm^2) Average value	E.I eff (kN/mm^2) Range[a]	Max. Bending moment at failure (kN.m) Average value	Max. Shear force at failure (kN) Average value	Failure mode
I	3	9491844591	500583991	166.6	83.3	Shear 67 % Bending 33%
IIa	3	9478629734	438614224	134.7	67.3	Shear 100 %
IIb	3	9799014933	576502703	177.9	89.0	Shear 67 % Bending 33%

[a] Range: difference between the maximum and minimum values obtained.

To manage the results shown for the bending specimens tested in the full-size panels, we divide the stiffness by the width of the specimen and then multiply by the actual real panel size.

Figure 8 represents the above results graphically for better comparison.

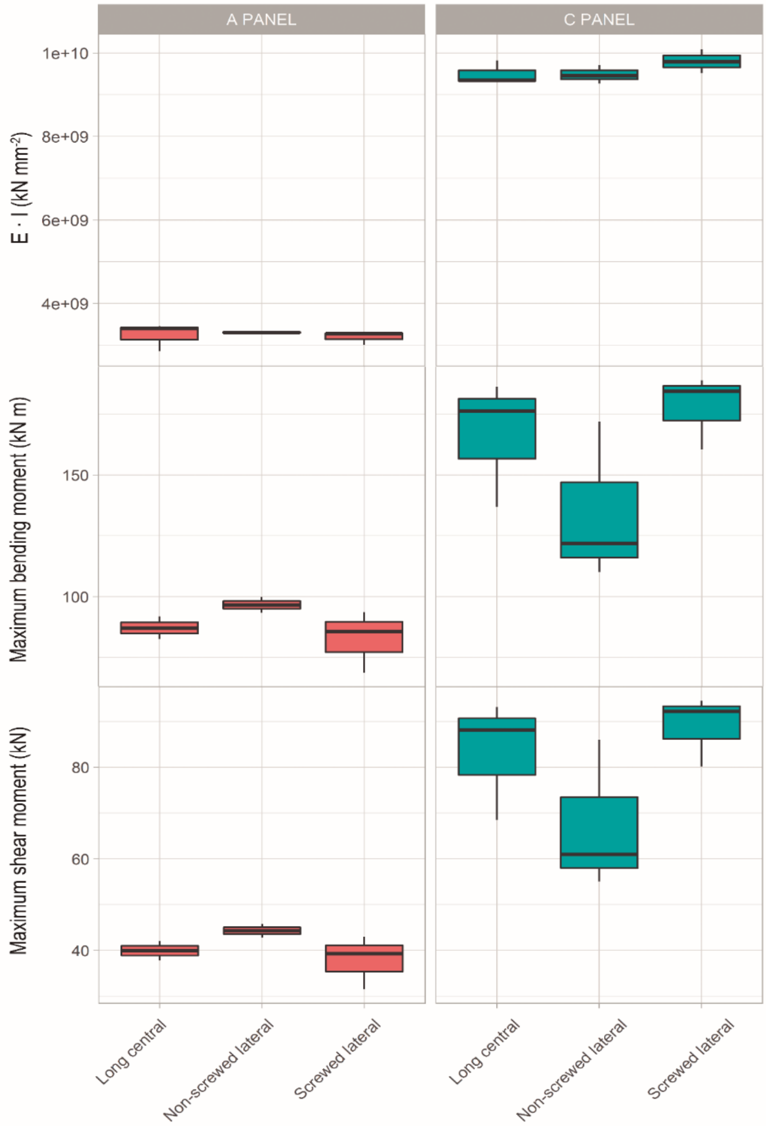

Figure 8. Bending stiffness (above), maximum bending moment at failure (centre) and maximum shear force at failure (below) obtained for the different specimens tested of 593 mm width.

ANOVA tests have been carried out to analyse if there are significant differences between the panels (A or C) and between the central (I) and lateral types (IIa and IIb). The results obtained show that there are no significant differences (p-value ≥ 0.05) between the parameters: bending stiffness, maximum bending moment and maximum shear moment in the same panel (A or B) and among the central, non-screwed lateral or screwed lateral tests (Table 4).

Table 4. ANOVA results for stiffness and shear to see considering type tests specimens (I, IIa, IIb)

Panel type	Parameter	P-value
A	Bending stiffness	0.8815
	Maximum bending moment	0.3054
	Maximum shear moment	0.3104
C	Bending stiffness	0.3162
	Maximum bending moment	0.1850

	Maximum shear moment	0.1849

Regarding the A panels:

- The stiffness of the different specimen types is similar in the mean values obtained, although the variability of the lateral non screwed specimens is lower as the other two types of specimens. It can be inferred for practical in situ use that the stiffness for the panel area of the central pair of ribs is like the one observed in the lateral double ribs, as it was expected.
- The bending moment and the shear moment shows certain variability in the obtained values. This seems to be due to specific lower load failures in some specimens caused by the manufacturing processes.
- Most of the failures are of bending but a considerable percentage of shear failures are also present, although results do not show significant differences among them. Considering this, we can remark the importance of paying attention on careful manufacturing process of this kind of products.

Regarding the C panels:

- Again, the behaviour of stiffness is very similar in the three types of specimens tested, showing that the area of the central pair of ribs is according to the one observed in the lateral double ribs.
- The bending moment and the shear moment show variability in the values that, after analysis, seem again to be due to manufacturing issues.
- Most of the failures are of shear between stringer and CLT, and less of them produced by bending. C panels require additional glue process for the above CLT layer. These results are according the manufacturing process.

Considering the obtained results, the panels' stiffness can be taken as the one obtained with the specimens of type I, while the panels' strength must be evaluated using the lower values obtained in all specimen types.

3.2. Comparison of the experimental stiffness with the predicted values using the Gamma Method

Table 5 shows the comparison of the average value for the stiffness obtained in the tests of type I with the results of the Gamma Method for CLT modified for SSPs for the full geometry of the specimen.

Table 5. Comparison of experimental and theoretical values for the stiffness of the C panels

Specimen Dimensions (mm)	E.I eff (N/mm^2) Average value Test spec. type I (1)	E.I eff (N/mm^2) Estimated value Gamma Method (2)	Ratio (2)/(1)

b: 593 h: 320 L: 6000	$9.49184 \cdot 10^{12}$	$8.26766 \cdot 10^{12}$	0.87

The result of the comparison shows that the use of the Gamma Method with the proposed methodology, including the use of the actual width of the specimen instead as the effective width, derives on conservative although acceptable values for the tested span and product, being the theoretical value 87 % of the one obtained from the tests.

3.3. Efficiency in use of wood compared to CLT equivalent elements

The experimental values of stiffness obtained for both panels (A and C) were compared with CLT elements equivalent in stiffness. The definition of these equivalent CLT elements was made using the Gamma Method for CLT elements according to Gagnon and Popovski (2011) methodology.

Once the equivalent CLT sections were defined, the amount of wood used in the A and C SSPs were compared with those of the CLT sections, considering only the final timber constituting the element and therefore, not including planning material losses. The results are shown in Table 6.

Table 6. Comparison among the net use of timber in A and C panels and CLT elements of similar stiffness

Panel type	Description	E.I eff ($kN\ mm^{-2}$) Average	Use of wood (m^3/specimen of 1 m)
A	200-60	$3.23613 \cdot 10^{12}$	0.690
CLT 220	43-43-43-43-43	$3.21687 \cdot 10^{12}$	1.584
CLT 224	32-32-32-32-32-32-32	$3.39591 \cdot 10^{12}$	1.613
C	60-200-60	$9.49180 \cdot 10^{12}$	1.126
CLT 319	46+45+46+45+46+45+46	$9.44086 \cdot 10^{12}$	2.297

The results show that the use of the proposed CLT-SSP panels A and C will lead to using a smaller amount of wood, which can be estimated up to 43% for the roof A panel and up to 49% for the floor C panel.

4. CONCLUSIONS

The tests and theorical assessment of the new system designed of SSPs based on CLT using *Pinus uncinata* wood show adequate mechanical values for the expected mechanical performance, both for the roof elements (panel A) as for the floor elements (panel C). The Gamma method proposed for modelling stiffness of the panels designed is compatible and produces conservative values for the real tested situation. In addition, the comparison with CLT elements of similar stiffness shows a significant saving in the use of wood, increasing the material efficiency.

This result will allow valorising and wisely using this alternative resource, promoting at the same time the development of the forest areas in which *Pinus uncinata* species is growing. Finally, these systems of panels intend to incorporate cork as insulation material, providing an alternative based on natural and renewable materials available in Southwestern Europe and contributing to the development of local economies in rural less-favoured regions based on sustainable wood-based construction.

ACKNOWLEDGEMENTS

This research was supported by the project IMIP - Innovative Eco-construction System based on Interlocking Modular Insulation Wood & Cork-based Panels (2020-2023). The IMIP project is co-financed by the Interreg SUDOE program of the European Union and the European Regional Development Fund (ERDF). We also thank the company FUSTES SEBASTIÁ S.L. in Rialp, Lleida (Spain) for manufacturing the SSP and CLT panels.

REFERENCES

Brunet-Navarro, P.; Gilabert, S.; Monleón, M.; Redón, M.; Hermoso, E.; Sánchez-González, M.; Luengo, E.; Mandrara, Z.; Gominho, J. and Oliver-Villanueva, J.V. (2020) Interlocking Modular Insulation Panels Manufactured with Mediterranean Pinewood and Cork. Environ. Sci. Proc. 2021, 3, 86-90.

Burgers, A.; Montero, C.; Gené Sera, J..; Vilches Casals, M.; Modol, E.; Langbour, P.; Thibaut, B. (2019) Timber grading of Pinus uncinata, a lesser-known pine species from the pyrenean mountain range. Maderas Ciencia y Tecnología 21 (2): 261-276.

Cantegrel, R. (1981). Contribution à l'étude de la variabilité biologique et biochimique du pin à crochets (*Pinus uncinata* Ram.) dans les pyrénées. Ann. Sci. For., 41 (3), 273-302.

Christophe C., Lopez-Saez, J., Stoffel, M., Rovéra, G., Edouard, J.L., Guibal, F. (2015). Impacts of more frequent droughts on a relict low-altitude *Pinus uncinata* stand in the French Alps. Front. Ecol. Evol., 20 January 2015. Sec. Paleoecology. Volume 2 – 2014. https://doi.org/10.3389/fevo.2014.00082

Choi, C., Kojima, E., Kim, K.-J., Yamasaki, M., Sasaki, Y., & Kang, S.-G. (2018). Analysis of Mechanical Properties of Cross-laminated Timber (CLT) with Plywood using Korean Larch. BioResources, 13(2), 2715–2726.

Darzi, S., Karampour, H., Bailleres, H., Gilbert, B. P., & McGavin, R. L. (2020). Experimental study on bending and shear behaviours of composite timber sandwich panels. Construction and Building Materials, 259, 119723.

DB-SE (2019) Documento Básico de Seguridad Estructural. Ministerio de Fomento. Dirección General de Arquitectura, Vivienda y Suelo. Spain.

DB-SE-AE (2009) Documento Básico de Seguridad Estructural. Ministerio de Fomento. Dirección General de Arquitectura, Vivienda y Suelo. Spain.

De Araujo, V., Aguiar, F., Jardim, P., Mascarenhas, F., Marini, L., Aquino, V., Santos, H., Panzera, T., Lahr, F., Christoforo, A. (2023), Is Cross-Laminated Timber (CLT) a Wood Panel, a Building, or a Construction System? A Systematic Review on Its Functions, Characteristics, Performances, and Applications. Forests 2023, 14(2), 264; https://doi.org/10.3390/f14020264

Dong, W., Wang, Z., Zhou, J., & Gong, M. (2021). Experimental study on bending properties of cross-laminated timber-bamboo composites. Construction and Building Materials, 300, 124313.

EN 338 (2016). Structural timber - Strength classes. European Committee for Standardization, CEN, Brussels, Belgium, 2016

EN 408 (2010+A1:2012) Timber structures - Structural timber and glued laminated timber - Determination of some physical and mechanical properties. European Committee for Standardization, CEN, Brussels, Belgium, 2012.

EN 1995-1-1 (2004+AC:2006+A1:2008+A2:2014) Eurocode 5: Design of timber structures - Part 1-1: General - Common rules and rules for buildings. European Comitee for Standarditazion, CEN, Brussels, Belgium, 2016.

EN 13170 (2012+A1:2015). Thermal insulation products for buildings - Factory made products of expanded cork (ICB) – Specification. European Comitee for Standarditazion, CEN, Brussels, Belgium, 2015.

EN 15425 (2017) Adhesives - One component polyurethane (PUR) for load-bearing timber structures - Classification and performance requirements. European Comitee for Standarditazion, CEN, Brussels, Belgium, 2013.

EN 16351 (2021) Timber structures - Cross laminated timber – Requirements. European Comitee for Standarditazion, CEN, Brussels, Belgium, 2021.

Gagnon, S., Popovski, M. (2011) CLT Handbook, Chapter 3 - Structural Design of crosslaminated timber elements. FPinnovatons Special Publication SP-528E. Quebec, Canada.

Hami, B., Irekti, A., Aribi, C., Bezzazi, B., & Mir, A. (2014). Experimental study of sandwich multilayer reinforced by glass fibre and agglomerated cork. Advanced Composites Letters, 23(5), 121–125.

IMIP (2023). EU Project INTERREG SUDOE – Innovative Eco-construction System based on Interlocking Modular Insulation Wood&Cork-based Panels. www.sudoe-imip.eu

Lakreb N, Knapic S, Saporiti S, Bezzazi B, Pereira H (2018) Properties of multilayered sandwich panels with an agglomerated cork core for interior applications in buildings. Eur. J. Wood Prod. 76, 143–153.

Lavrencic, M., & Brank, B. (2018). Failure analysis of ribbed cross-laminated timber plates. Coupled Systems Mechanics, 7(1), 79–93.

LIFE21-NAT-ES-LIFE UNCINATA (2023). EU Project LIFE21-NAT-ES-LIFE UNCINATA/101074730 2022-2027. Restoration, conservation, and resilience of mountain pine (*Pinus uncinata*) forests on limestone in the Pyrenees. https://webgate.ec.europa.eu/life/publicWebsite/project/details/101074730

López Díez, M.E., Martinez Garcia, F., Postigo Mijarra, J.M. (2011). *Pinus uncinata* Ramond ex DC.: Conservation and proposal of management at its southwestern limit of distribution In: "4th International Conference on Mediterranean Pines, mEDPINE 4", 06/06/2011 - 10/06/2011, Avignon, France (https://oa.upm.es/12523/)

Loss, C., & Davison, B. (2017). Innovative composite steel-timber floors with prefabricated modular components. Engineering Structures, 132, 695–713.

Luengo, E., Hermoso, E., Cabrero, J.C., Arriaga, F. (2017) Bonding strength test method assessment for Cross-Laminated Timber Derived Stressed-Skin Panels (CLT SSP). Materials and Structures 50, 204.

Munis, R. A., Camargo, D. A., de Almeida, A. C., de Araujo, V. A., Lima Junior, M. P. de, Morales, E. A. M., Simões, D., Biazzon, J. C., de Matos, C. A. O., & Cortez-Barbosa, J. (2018). Parallel Compression to Grain and Stiffness of Cross Laminated Timber Panels with Bamboo Reinforcement. BioResources, 13(2), 3809–3816.

NF-B 52-001-1 (2011 & 2018) Règles d’utilisation du bois dans la construction — Classement visuel pour l’emploi en structures des bois sciés résineux et feuillus — Partie 1 : Bois massif. AFNOR, La Plaine St-Denis, France.

Santos, P., Correia, J. R., Godinho, L., Dias, A. M. P. G., & Craveiro, H. (2021). Experimental and numerical assessment of a cross-insulated timber panel solution. Engineering Structures, 235, 112061

Shahnewaz, M., Dickof, C., Zhou, J., & Tannert, T. (2022). Vibration and flexural performance of cross-laminated timber – glulam composite floors. Composite Structures, 292, 115682.

Stanić, A., Hudobivnik, B., & Brank, B. (2016). Economic-design optimization of cross laminated timber plates with ribs. Composite Structures, 154, 527–537.

UNCI´PLUS (2011). EU Project INTERREG. http://www.unciplus.eu/copy_of_presentation-generale-du-projet

UNE 56544 (2011 & 2022) Clasificación visual de la madera aserrada para uso estructural. Madera de coníferas. AENOR, Madrid, Spain.

UNE 56920 (1990). Granulados de corcho. Especificaciones. AENOR, Madrid, Spain, 1990.

Wei, P., Wang, B. J., Li, H., Wang, L., Gong, Y., & Huang, S. (2021). Performance Evaluation of a Novel Cross-laminated Timber Made from Flattened Bamboo and Wood Lumber. Bioresources, 16(3), 5187–5202.